INTERACTION OF A SEVERELY UNDEREXPANDED GAS STREAM ISSUING FROM A CYLINDRICAL CHANNEL WITH AN ADJACENT SURFACE

A. V. Beloshitskii, E. N. Bondarev,
E. N. Voznesenskii, V. I. Nemchenko,
and N. A. Samsonov

UDC 533.6.011

We will examine the discharge of a gas through a cylindrical channel into a low-pressure medium or vacuum in the Reynolds number range 100-15000 in the presence of a flat boundary surface passing across the outlet section of the channel. We obtain the distribution of the gasdynanic parameters in the outlet section and in the peripheral part of the stream and the pressure distribution over the boundary surface.

It is known that a stream of ideal gas issuing from a sonic nozzle into a vacuum or a medium with sufficiently low pressure exerts a strong action on a flat surface which crosses the outlet section of the nozzle perpendicular to its axis. This action is intensified when the gas is viscous. Here, a boundary layer develops on the surface adjacent to the orifice and additionally limits expansion of the stream. The flow pattern is complicated considerably if the viscous gas is discharged from a channel of finite length, in which case a boundary layer develops within the channel. This is accompanied by the formation of a "fluid nozzle" near the outlet section of the channel, with low supersonic Mach numbers in the plane of its edge and substantial flow nonuniformity [1-4], which leads to a change in the structure of the stream and its interaction with the surface.

The present article reports results of generalization of a numerical and experimental study of the problem of the motion of a viscous gas in a channel of finite length and its interaction with an adjacent surface when discharged into a vacuum or low-pressure space. The numerical study [1] was conducted within the framework of the Navier–Stokes equations.

1. We will examine the problem of the steady-state motion of a viscous, heat-conducting gas in a cylindrical channel of constant cross section when the gas is discharged into a vacuum in the presence of a boundary surface passing across the outlet section of the channel.

Figure 1a presents a diagram of the region being studied. It includes the channel from the inlet section OA to its outlet BB' and part of the medium B'BCDE. The external region is bounded by the outlet section of the channel BB', the solid surface BC adjacent to the channel edge, and a cylindrical surface CDE located distances Δx and Δy from the outlet section of the channel and the symmetry axis, respectively.

According to the presently available data [2-4], the physical pattern of discharge into a vacuum from a sufficiently long channel can be represented as follows: As the viscous gas moves along the channel wall, a boundary layer develops. Development of the boundary layer leads to a decrease in the effective through section, shifting of the streamlines toward the axis, and acceleration of the subsonic flow. At the same time, perturbations propagate from the low-pressure medium counter to the flow along the boundary layer on the other side of the channel and impede its development. The velocity profile is filled out beginning with a certain distance from the inlet, and the effective through cross section of the channel increases as the outlet edge of the channel is approached. The streamlines in the channel form a Laval nozzle with a fluid contour, and the flow velocity on the axis inside the channel reaches the sonic velocity and subsequently becomes supersonic.

The nonuniform flow formed in the channel and the boundary layer growing beyond the channel edge along the surface GC will determine the flow properties of the stream — particularly its peripheral part.

The fact that the internal flow in the channel and the flow outside the channel affect each other makes it necessary to calculate them simultaneously.

Moscow. Translated from Zhurnal Prikladnoi Mekhaniki i Tekhnicheskoi Fiziki, No. 2, pp. 121-128, March-April, 1985. Original article submitted February 13, 1984.

 0021-8944/85/2602-0262$09.50

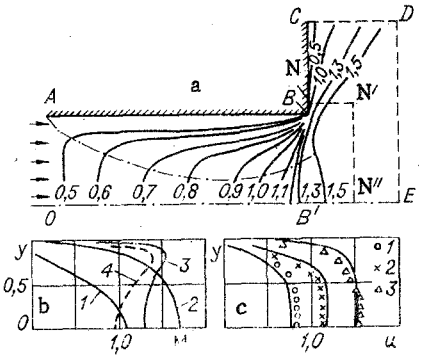

Fig. 1

The system of Navier–Stokes equations for a compressible gas in a cylindrical coordinate system is written as follows:

$$\frac{\partial \rho}{\partial t}+u\frac{\partial \rho}{\partial x}+v\frac{\partial \rho}{\partial y}+\rho\left(\frac{\partial u}{\partial x}+\frac{1}{y}\frac{\partial}{\partial y}yv\right)=0,$$

$$\frac{\partial u}{\partial t}+u\frac{\partial u}{\partial x}+v\frac{\partial u}{\partial y}+(\gamma-1)\left(\frac{e}{\rho}\frac{\partial \rho}{\partial x}+\frac{\partial e}{\partial x}\right)=\frac{1}{\mathrm{Re}\,\rho}\left\{\frac{4}{3}\frac{\partial}{\partial x}\mu\frac{\partial u}{\partial x}+\frac{1}{y}\frac{\partial}{\partial y}\mu y\frac{\partial u}{\partial y}+F_u\right\},$$

$$\frac{\partial v}{\partial t}+u\frac{\partial v}{\partial x}+v\frac{\partial v}{\partial y}+(\gamma-1)\left(\frac{e}{\rho}\frac{\partial \rho}{\partial y}+\frac{\partial e}{\partial y}\right)=\frac{1}{\mathrm{Re}\,\rho}\left\{\frac{\partial}{\partial x}\mu\frac{\partial v}{\partial x}+\frac{4}{3}y\frac{\partial}{\partial y}\mu y\frac{\partial v}{\partial y}+F_v\right\},$$

$$\frac{\partial e}{\partial t}+u\frac{\partial e}{\partial x}+v\frac{\partial e}{\partial y}+(\gamma-1)e\left(\frac{\partial u}{\partial x}+\frac{1}{y}\frac{\partial}{\partial y}yv\right)=\frac{1}{\mathrm{Re}\,\rho}\left\{\frac{\gamma}{\mathrm{Pr}}\left[\frac{\partial}{\partial x}\mu\frac{\partial e}{\partial x}+\right.\right. \tag{1.1}$$

$$\left.\left.+\frac{1}{y}\frac{\partial}{\partial y}\mu y\frac{\partial e}{\partial y}\right]+\Phi\right\},$$

$$F_u=\frac{1}{y}\left[\frac{\partial}{\partial y}\mu y\frac{\partial v}{\partial x}-\frac{2}{3}\frac{\partial}{\partial x}\mu\frac{\partial}{\partial y}yv\right],\quad F_v=\frac{\partial}{\partial x}\mu\frac{\partial u}{\partial y}-\frac{2}{3}\frac{\partial}{\partial y}\mu\frac{\partial u}{\partial x}-\frac{2\mu v}{y^2}-\frac{2}{3}v\frac{\partial}{\partial y}\frac{\mu}{y},$$

$$\Phi=\mu\left\{2\left[\left(\frac{\partial u}{\partial x}\right)^2+\left(\frac{\partial v}{\partial y}\right)^2+\frac{v^2}{y^2}\right]-\frac{2}{3}\left(\frac{\partial u}{\partial x}+\frac{1}{y}\frac{\partial v}{\partial y}\right)^2+\left(\frac{\partial u}{\partial y}+\frac{\partial v}{\partial x}\right)^2\right\}$$

(all of the notation is conventional).

In forming the dimensionless variables, we referred the geometric quantities to the channel radius and the flow parameters to the critical parametes. In solving the internal problem together with calculation of the flow in the vicinity of the channel outlet, we placed the origin of the coordinates at the point of intersection of the symmetry axis with the inlet plane. In the external problem, the origin was located at the intersection of the symmetry axis and the outlet plane of the channel.

Since we are studying the discharge of gas from a channel into a vacuum, its movement in the channel occurs with a limiting pressure drop, and each set of characteristic parameters (Reynolds number, channel length L, temperature factor, etc.) corresponds to a certain rate of flow through the channel. This flow rate should be determined during the calculation. The gasdynamic parameters in the inlet section will be determined from the equation of flow rate in the inlet and outlet sections for steady-state conditions and the known value of the total energy and entropy.

Thus, on the boundary OA we write the following boundary conditions:

$$\frac{u^2}{2}+\frac{\gamma}{\gamma-1}\frac{p}{\rho}=\frac{u_*^2}{2}+\frac{\gamma}{\gamma-1}\frac{p_*}{\rho_*},\quad \frac{p}{\rho^\gamma}=\frac{p_*}{\rho_*^\gamma},$$

$$\int_0^1 \rho u y dy\,|_{x=0}=\int_0^1 \rho u y dy\,|_{x=L},\quad v=0.$$

Here, u and v are components of velocity along the x and y axes, respectively; x = 0 is the inlet section of the channel; x = L is the outlet section of the channel; the asterisk denotes critical values.

Conditions of flow adhesion and the surface temperature T_w are prescribed on the channel wall AB. The density is determined from the condition of triviality of the pressure gradient along a normal to the solid surface. The following flow symmetry conditions will be used on the symmetrix axis OE:

$$v = \partial u/\partial y = \partial \rho/\partial y = \partial e/\partial y = 0. \tag{1.2}$$

In accordance with the conditions of the problem, gas flows out of the region being examined on the top and right boundaries CD and DE, which allows us to use the condition of "free discharge:"

$$\partial^2 f_i/\partial n^2 = 0,\ f_i = \{\rho,\ u,\ v,\ e\}.$$

One of the following conditions is postulated along the solid surface BC:
a) condition of flow adhesion

$$u = v = 0,\ T_w = \text{const},\ \partial p/\partial n = 0; \tag{1.3}$$

b) conditions of absence of friction on the surface

$$u = 0,\ \partial v/\partial n = \partial e/\partial n = \partial \rho/\partial n = 0; \tag{1.4}$$

c) conditions of flow slip

$$\psi = 0,\ \partial p/\partial n = 0,\ v(0) = \frac{2-\sigma}{\sigma}\lambda\left(\frac{\partial v}{\partial x}\right)_{x=L} + \frac{3}{4}\frac{\mu}{\rho T}\left(\frac{\partial T}{\partial y}\right)_{x=L},$$
$$T(0) - T_w = \frac{2-\alpha}{\alpha}\frac{2\gamma}{\gamma+1}\frac{\lambda}{\mathrm{Pr}}\left(\frac{\partial T}{\partial x}\right)_{x=L}, \tag{1.5}$$

where σ is part of the diffusively reflected molecules ($\sigma = 1$); α is the accommodation factor ($\alpha = 1$); λ is the mean free path of the molecules $\lambda = 1.26\sqrt{\gamma}(\mu/\rho\alpha)$.

We used the following initial conditions in the calculations. In the channel OABB' we specified a uniform sonic flow. In the external medium we specified a parameter distribution corresponding to flow from a source. A steady-state solution was obtained.

The initial system of differential equations (1.1) was approximated by means of an implicit difference scheme by the decomposition method proposed in [5]. The region of integration was covered by a nonuniform rectangular difference grid. We employed logarithmic condensation of the grid around the channel wall and near its outlet section.

Viscosity was evaluated by calculating the flow in the boundary layer of a cooled plate. Comparison of the results of the calculations at $\mathrm{Re} \leq 5 \cdot 10^5$ with the solution of the boundary-layer equations in [6] showed that they agreed satisfactorily. Thus, the viscosity in the theoretical scheme is small compared to the actual viscosity in this range of Reynolds numbers. Calculations of gas flow in the channel showed satisfactory convergence of the solution with the change in the steps of the difference grid and the absence of an effect by the chosen position of the boundaries CD and DE ($\Delta x = 2$, $\Delta y = 1.5$) on flow in the channel.

To eliminate the effect of approximation errors occurring in calculation of flow about the edge of the outlet section of the channel, we refined the solution for flow in the stream by calculating the turning of the flow around the right angle on a denser grid.

2. Figure 1a shows a typical flow pattern in the channel for the case L = 10, Re = 200, and $T_w = 1$ obtained in the calculation. The solid lines represent lines of equal Mach numbers, the dot-dash lines represent the boundary of the boundary layer, and the dashed lines represent the nominal boundaries of the integration region. The flow features are the presence of a sonic surface extending into the channel and a supersonic flow velocity across nearly the entire outlet section except for a small annular region near the angled edge. The Mach number on the axis of the outlet section $M \sim 1.3$. In the internal region of flow between the boundary of the boundary layer and the symmetry axis in the channel, the lines of equal Mach numbers ($M < 1$) are nearly perpendicular to the longitudinal axis. In the boundary layer, these lines converge toward the angled edge of the outlet section due to stagnation of the flow.

The pressure is practically constant in the cross sections in the middle part of the channel. However, at low Reynolds numbers ($\lesssim 250$), the calculations revealed a small increase in pressure (up to 10%) near the wall around the inlet section of the channel. A transverse

pressure gradient appears in those sections where the speed of sound has been reached on the channel axis. Pressure becomes less on the wall than on the axis. As we move toward the outlet section, we see the pressure drop between the axis and wall increase and reach about 30% at the channel outlet.

It was shown in [3] that, given identical conditions at the channel inlet, the parameter's distribution in it depends on the coordinate x/Re. The completed calculations showed that for the case of discharge of the gas into a vacuum the parameter x/Re can also serve as a gas-flow similarity parameter for sufficiently long channels.

Characteristic distributions of the Mach number in the outlet section corresponding to different values of L/Re are shown in Fig. 1b, where curves 1-3 at L = 10 correspond to L/Re = 0.5; 0.06; 0.002; curve 4 at L = 0.5 corresponds to L/Re = 0.002.

In the case when the boundary layer fills the entire channel, the distribution of the Mach numbers in the outlet section is nearly parabolic. The maximum velocity over this section is reached on the axis at M ~ 1. A decrease in the parameter L/Re from 0.5 to 0.06-0.07 leads to an increase in the Mach number on the channel axis. The character of the Mach number distribution remains the same, but the profile becomes fuller. Here, the maximum Mach number on the axis of a sufficiently long channel is 1.35 and is realized at a value of L/Re ~ 0.06-0.07. This flow regime is characterized by the beginning of union of the external boundaries of the boundary layer near the outlet section of the channel.

A further decrease in L/Re < 0.07 leads to a nonmonotonic Mach-number distribution in the outlet section, and the maximum value of M over the section is reached in the peripheral part of the flow (see curve 3 in Fig. 1b). The flow velocity is supersonic over nearly the entire outlet section.

The completed calculations show that with short channels the Mach-number distribution in the outlet section depends on channel length with a constant value of L/Re. A decrease in channel length leads to a decrease in the Mach number, particularly in the vicinity of the symmetry axis. Figure 1b shows the distribution of M in the outlet section of the channel with L/Re = 0.002 and different lengths (curves 3 and 4). We should point out the presence of the subsonic section of flow in the vicinity of the symmetry axis with L = 0.5. The calculations show that channel length has the greatest effect on the distribution of gasdynamic parameters in the outlet section of the channel when L < 2.

The results of numerical calculation of gas flow in the channel were compared with experimental data in [4]. The conditions of the experiment in [4] differed from the formulation of the problem in the numerical study [1] only in the fact that in the experiment the inlet section was constructed in accordance with Vitoshinskii, which made it possible to form an attached flow at the channel inlet. However, there is a boundary layer here. Figure 1c compares the calculated and experimental distributions of velocity in cross sections of the channel with L = 10, Re = 492, and $T_w = 1.23$, where points 1-3 correspond to x = 6.4, 9, and 10; the solid lines correspond to the calculated results. The calculated and empirical data agree adequately. Some discrepancy is seen in the outlet section, where the errors of the studies are greatest due to the complexity of the flow.

3. We studied the flow field of the stream for the above-obtained characteristic distributions of gasdynamic parameters at the channel edge. To exclude the effect of approximation errors accumulated in the numerical experiment near the edge on the results of calculations of flow in the stream, the above-described theoretical region and boundary conditions were modified as follows: inside the integration region OABCDE near the outlet section of the channel in the external medium we introduced the cylindrical surface NN'N". This surface is located a distance $\Delta x = 0.5$ from the channel edge along the Ox axis and a distance $\Delta y = 0.1$ from point B along the Oy axis (see Fig. 1a). Gas flow in the stream was calculated within the region NCDEN"N'. The boundary conditions on the surfaces NC, CD, and DE and the line EN" were prescribed in accordance with the scheme (1.2-1.5), while the distributions of gasdynamic parameters obtained in calculating discharge of the gas through the channel served as the boundary conditions on the surfaces NN' and N'N". In the boundary layers of the flow on the surface NN' the distributions were refined by performing additional calculations on a denser difference grid for the rotation of the nonuniform flow formed in the channel near the right angle.

The dimensions of the theoretical field along the x and y coordinates were 20 and 25 channel radii, respectively. To check the correctness of the method, we calculated the flow

field of a stream flowing into a vacuum from a sonic nozzle with a uniform parameters distribution in the outlet section at Re = 10^7. The results here agreed satisfactorily with the calculated data in [7] corresponding to flow of an ideal gas.

Let us examine the effect of nonuniformity of the parameters in the outlet section of the channel on the flow field of the stream. Figure 2a shows the position of lines of equal Mach numbers in the field of the stream obtained under different conditions at the channel edge. Curves 1 were obtained with a uniform sonic flow in the outlet section. Curves 2 were obtained with a parameter distribution corresponding to a channel with L/Re = 0.002, while curves 3 were obtained for a channel with L/Re = 0.06, Re = 10^7. We postulated conditions of stationariness of the flow along the surface BC and the absence of friction on the wall. With the given boundary conditions, the differencesin the flow field of the stream are due to the nonuniformity of the distribution of the gasdynamic parameters in the outlet section of the channel. It is apparent from Fig. 2a that due to loss in the boundary layer of the channel, the lines M = const in the peripheral part of the stream are farther from the channel edge than in the case of ideal gas flow. The effect of nonuniformity of the parameters at the channel outlet is manifest at distances x < 5 from the edge near the stream axis. Figure 2b shows lines of equal Mach numbers (the dot-dash lines) in a stream issuing from a channel characterized by the ratio L/Re = 0.002 at Re = 5000. The calculations were performed using conditions of slip (1.5) along the surface BC. The decelerating effect of the boundary layer, which increases in size beyond the edge of the outlet section along the surface BC, keeps the lines of equal Mach numbers in the peripheral part of the stream from reaching BC. Insteady, they diverge at a certain angle relative to this surface. Allowing for conditions of flow slip has a significant effect on the position of the lines M = const. Flow in the peripheral part of the stream is characterized by a rapid decrease in density with increasing distance from the channel edge in the plane of its outlet section, which corresponds to a decrease in the local Reynolds number and leads to a rapid increase in the thickness of the boundary layer. The position of the external boundary of the boundary layer obtained in the calculation with L/Re = 0.002, Re = 5000 and slip conditions is shown in Fig. 2b by the dashed line. The solid lines represent isobars. Within the region being discussed the boundary layers grows according to the relation $\delta \sim y^{1.1}$ (δ is the thickness of the boundary layer and y is the coordinate along the surface BC). It can be seen from Fig. 2b that the pressure is practically constant across the boundary layer. To check the results of calculation of the stream field, we studied the distribution of the pressure associated with the total head p_0' using total-head probes (with a diameter $d_1 = 6.5 \cdot 10^{-3}$, $d_2 = 2.2 \cdot 10^{-2}$ m). This made it possible to calculate the distribution of the numbers M along the axis (Fig. 2c) both for long channels L = 12 and for very short channels L = 0.12 (conical inlet), L/Re = $5.61 \cdot 10^{-5}$; $3.64 \cdot 10^{-5}$; $2.43 \cdot 10^{-5}$ (L = 12, points 1-3, smooth inlet); $5.61 \cdot 10^{-3}$; $3.64 \cdot 10^{-3}$; $2.43 \cdot 10^{-3}$ (points 4-6). The solid line represents results of calculation of the Mach number distribution along the stream axis with L = 10, L/Re = 0.002, and Re = 5000. It must be noted that at $x \leq 0.5$, the distance of the exit of the shock from the probe is comparable to the distance from the end of the nozzle to the surface of the wall. In this region, it is difficult to evaluate the error of measurement of p'_0 and the subsequent determination of M. In the remaining part of the stream, at x > 0.5, the error of the Mach number is no greater than 5%.

In the discharge of the stream from a long channel L = 12, nearly all of the experimental results regarding the distribution of M along the stream axis at $x \geq 5$ agree satisfactorily with each other and with the results of calculation of the distribution of M along the axis both for discharge from a sonic nozzle and for discharge from a channel with L = 10, L/Re = $2 \cdot 10^{-3}$. In the case of a very short channel (L = 0.12 << 2), when the study results show the channel length has the greatest effect on the parameters at the edge of the channel, the distribution of M for moderate Re and L/Re $\approx 10^{-5}$-10^{-4} at x > 5 agrees well with the results of calculation of the flow field in the case of discharge from a long channel and a sonic nozzle. There is some increase in the Mach numbers on the stream axis with an increase in Re. The above results confirm the theoretical conclusion that nonuniformity of the distribution of the parameters at the outlet of the channel due to the effect of its length is manifest mainly near the edge.

However, even at $2 \leq x \leq 5$ and with a substantial difference in L (L = 0.12 and L = 12), there are no large differences in the experimental data for the range of numbers L/Re = $2.43 \cdot 10^{-3}$-$2.43 \cdot 10^{-5}$ and different geometries of channel inlet. The results are layered within the range 12-25% right near the outlet edge of the channel, but this requires additional study by more exact methods.

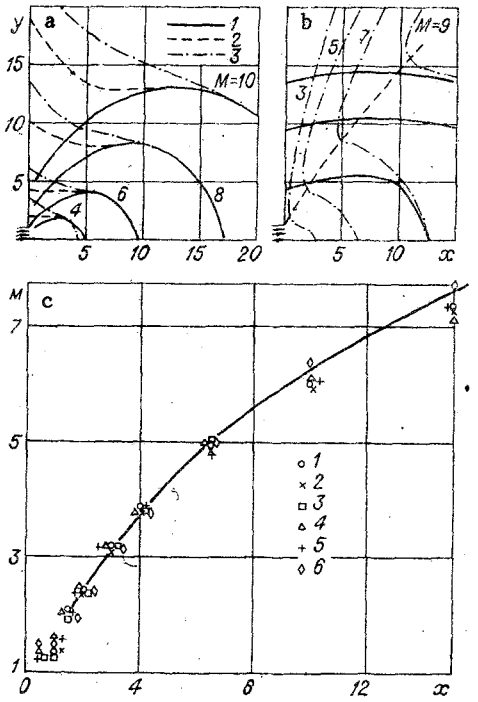

Fig. 2

Thus, with large L, the theory gives a distribution of M along the stream which is very close to the actual distribution. Flow nonuniformity at the channel outlet leads to a slight redistribution of M along the stream axis near the edge.

4. A stream issuing from a channel into a half-space with a reduced pressure has a strong effect on the boundary surface passing across its outlet section. The results of theoretical and experimental study of the pressure distribution along the adjacent surface are shown in Fig. 3.

To more fully determine the laws governing the mechanical interaction of a severely underexpanded gas stream issuing from a channel at reduced pressures in the surrounding space, we will supplement the results of theoretical studies by using all of the empirical data on measurement of induced pressure on the wall presented in [8-10]. We also performed a series of measurements to obtain closer agreement between theory and experiment.

All of the measurements were obtained by the same method on a series of models of two types with different inlet configurations: a smooth inlet constructed in accordance with Vitoshinskii, and a conical inlet with a bend point at the transition to the cylindrical channel. The experimental method and the design of the models were detailed in [9]. The most interesting model was a channel with a wall having an annular gap to relieve the induced pressure on the wall. This model made it possible to measure induced pressure on the wall in the immediate vicinity of the edge of the outlet hole at distances $1.064 \leq y \leq 6$. In connection with the fact that the experiment was conducted on an evacuated wind tunnel with a pumping system of limited capacity, out of all of the empirical results obtained we took only those results not affected by external pressure in the working chamber of the tunnel.

The calculations of pressure on the wall can be performed with sufficient accuracy if the boundary conditions on the surface are known. In particular, Fig. 3 shows the pressure distribution obtained in calculations for a stream issuing from a channel with L = 10, Re = 5000, and different boundary conditions along the surface BC.

The results of calculations performed using slip conditions (1.5) agree best with the experimental data in Fig. 3a with $L/Re \approx 0.00205$, L = 10, and $y \geq 8$ (lines 1-3 show results of calculation using boundary conditions (1.3-1.5), line 4 corresponds to the theory of inviscid flow (nonflow); points 5-10 correspond to L/Re = 0.002; 0.0024; 0.0017; 0.00205; 0.004; 0.0003, L = 6; 9; 12; 5-36 (conical inlet).

At distances $y < 8$, the theory, with boundary conditions (1.5) gives somewhat overstated values of induced pressure. The experimental results obtained with L = 6-12 and $L/Re \approx 0.002$

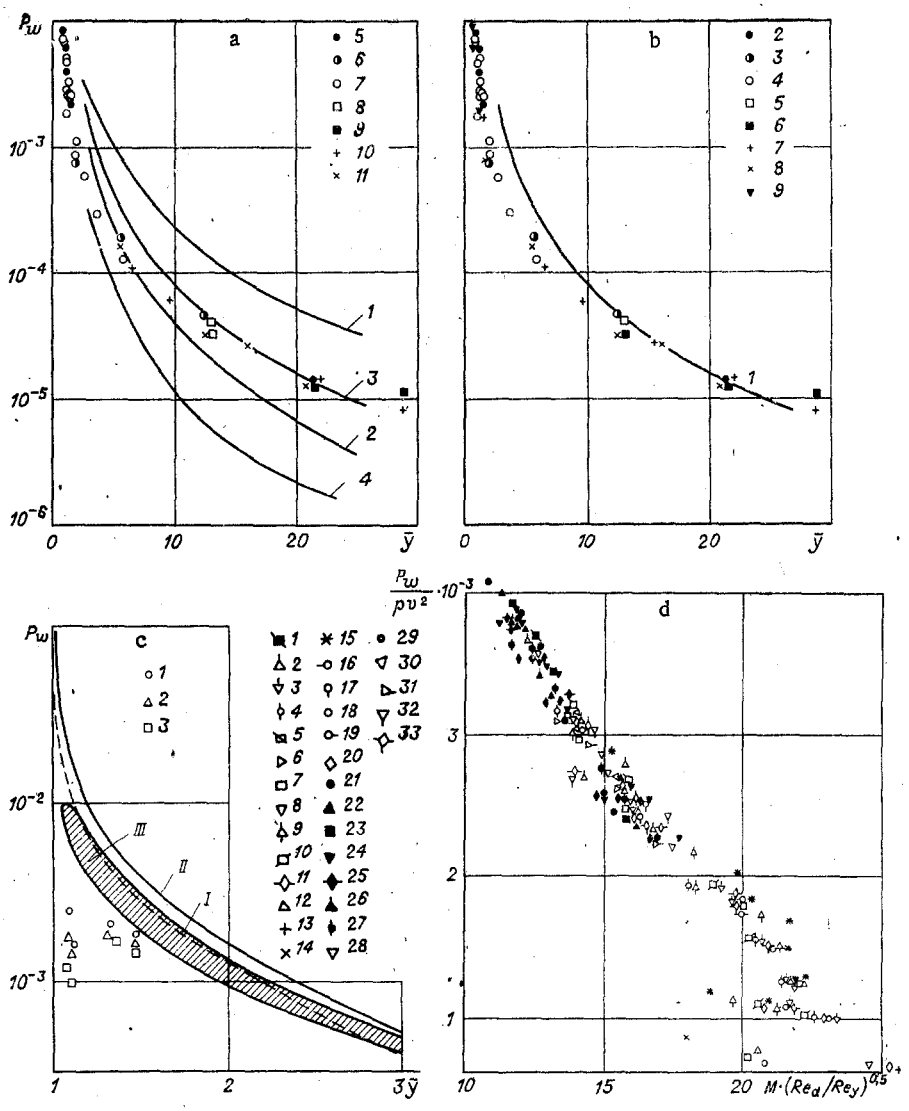

Fig. 3

form a single curve with scatter within the range 3-5% for channels with different inlet geometries. This shows that for long channels the effect of the initial conditions at the channel inlet lies within the limits of accuracy of the experiment and calculation. The results presented here are sufficient substantiation of the selection of a uniform velocity field at the channel inlet in the theoretical study. We should point out that in the immediate vicinity of the channel edge the pressure on the wall is more than one order greater than the pressure obtained from the Prandtl—Maier theory for sonic flow, while the pressure obtained in calculations with allowance for the effect of viscous forces is considerably greater than that obtained from the theory of inviscid flow (see Fig. 3a).

Figure 3b shows the effect of L/Re with long channels ($L \geq 2$) on the distribution of induced pressure on the wall, where the point 2 corresponds to L = 6, L/Re = 0.002 (smooth inlet), 3 corresponds to L = 9, L/Re = 0.0024 (conical inlet), 4 corresponds to L = 12, L/Re = 0.0017 (conical inlet), 5-8 correspond to L = 5-36, L/Re = 0.00205, 0.004, 0.0004, and 0.0003 (conical inlet), and 9 corresponds to L = 1.7-2.6, L/Re = 0.0008-0.0012 (conical inlet). The results shown indicate that the pressure distribution on the wall with discharge of the stream from a long channel is almost independent of the parameter L/Re if this quantity is less than 0.02. The experimental values of pressure on the wall in this case agree satisfactorily with the calculated results with L/Re = 0.002, L = 10 obtained with allowance for (1.5) (curve 1). Thus, with values of L/Re < 0.02 and L > 2, the flow changes to the limiting regime, when the dependence of the flow parameters on L/Re and L becomes extremely weak. No strong interaction was observed in the regime of completely viscous flow at L/Re < 0.1 in our investigation.

Figure 3b and c shows the effect of channel length and inlet geometry. At $L > 2$, the effect of channel length lies within the experiment error. With a decrease $L \leq 2$, such as $L = 2$, there is a decrease in pressure and some redistribution of pressure near the edge of the hole. However, it cannot be concluded that channel length has a significant effect from the experimental results for $L = 2$ and $L/Re \simeq 0.001$ (see Fig. 3b) obtained for short distances from the channel edge ($y = 1.086$-1.65).

Since the greatest pressure is seen in the region of the surface directly adjacent to the channel edge, we conducted a detailed theoretical and experimental study of the pressure distribution at distances $1 \leq y \leq 3$ (see Fig. 3c). The results of the theoretical calculations show that the same dependence of pressure on L/Re and L is seen near the outlet hole of the channel as at $y > 3$ (see Fig. 3c, curves I and II, $L = 10$ and 2, $L/Re = 0.067$ and 0.002, respectively). Pressure continues to increase with approach of the edge of the hole ($y \to 1$), exceeding the pressure calculated from the Prandtl—Maier theory by 2-3 orders of magnitude.

The results of experiments performed on a special model for $1.07 \leq y \leq 3$, a wide range $0.12 \leq L \leq 36$, and $1.97 \cdot 10^{-2} \leq L/Re \leq 1.27 \cdot 10^{-4}$ (curve III) shows that the effects of channel length and inlet geometry are not noticeable until $L \geq 0.36$ (points 1-3 in Fig. 3c are for $L = 0.12$, $L/Re = 5.68 \cdot 10^{-5}$; $3.69 \cdot 10^{-5}$; $2.46 \cdot 10^{-5}$). A decrease in L to 0.12 is accompanied by a sharp reduction in pressure near the hole edge to values close to the pressure values with rotation of a sonic flow through 90° at the edge in accordance with the Prandtl—Maier theory. Such behavior of induced pressure at $L \simeq 0.12$ can evidently be attributed to the fact that a decrease in channel length is accompanied by contraction of the stream inside the channel and termination of the sonic section at the edge of the hole. However, in this case as well, the geometry of the channel inlet does not affect the distribution of induced pressure.

The increase in induced pressure with $L = 0.12$ with increasing distance from the edge and the attainment of the maximum of induced pressure with an increase in y can be explained by the interaction of the inviscid flow with the boundary layer initiated on the wall.

The experimental data in Fig. 3 shows that at $L/Re < 0.02$-0.00005, the limiting value of induced pressure near the hole edge may be 15-20 times greater than the pressure value calculated from the Prandtl—Maier theory.

If we again compare the results of numerical and theoretical study of the flow, the results of the numerical study of the interaction with $L/Re = 0.002$ make it possible to conclude that pressure is constant across the boundary layer on the external wall. This finding confirms the hypothesis made in [10] regarding the constancy of pressure across the boundary layer for representation of induced pressure on the wall in the form of the relation $p/\rho v^2 = f(M\sqrt{Re_d/Re_y})$, which makes it possible to generalize all experimental data for Re_d - var and $0.5 \leq L \leq 30$ with a standard deviation on the order of 8-10%, regardless of the geometry of the inlet (Fig. 3d: L 0.62-30, $L/Re = 2.16 \cdot 10^{-5}$-$1.42 \cdot 10^{-2}$ (conical inlet) — points 1-20; L = 0.25-12 and $L/Re = 5.13 \cdot 10^{-5}$-$5.9 \cdot 10^{-2}$ (smooth inlet) — points 21-33).

The satisfactory generalization of the empirical data for small L/Re and different inlet geometries (see Fig. 3) and its satisfactory agreement with the numerical results obtained on the assumption of flow uniformity at the channel inlet show that, under these conditions, the effect of the inlet is negliglble.

On the whole, the above results of numerical and experimental study essentially characterize the discharge of a severaly underexpanded stream of a real gas from a cylindrical channel into a vacuum and its interaction with a flat wall adjacent to the edge of the channel.

The numerical method used to calculate flow throughout the region investigated gives results accurate enough for practical use.

LITERATURE CITED

1. A. V. Beloshitskii and E. N. Bondarev, "Discharge of a viscous gas from a cylindrical channel into a vacuum," Izv. Akad. Nauk SSSR Mekh. Zhidk. Gaza, No. 1 (1981).
2. M. E. Deich, Technical Gasdynamics [in Russian], Gosenergoizdat, Moscow (1961).
3. A. P. Byrkin and I. D. Mezhirov, "Calculation of a viscous gas flow in a channel," Izv. Akad. Nauk SSSR, Mekh. Zhidk. Gaza, No. 6 (1967).
4. Yu. G. Rakogon, "Some results of an experimental study of air flows in circular pipes at low Reynolds numbers," Tr. Mosk. Fiz. Tekh. Inst. (1974).

5. Yu. A. Berezin, V. M. Kovenya, and N. N. Yanenko, "Implicit scheme for calculating the flow of a viscous heat-conducting gas," ChMMSS, 3, No. 4 (1972).
6. L. G. Loitsyanskii, Mechanics of Liquids and Gases, Nauka, Moscow (1978).
7. V. A. Zhokhov and A. A. Khomutskii, "Atlas of supersonic flows of a freely expanding ideal gas leaving an axisymmetric nozzle," Tr. TsAGI, No. 1224 (1970).
8. E. N. Voznesenskii and V. I. Nemchenko, "Pressure distribution on the surface of a plate with concentrated injection," Tr. Mosk. Fiz. Tekh. Inst. (1973).
9. E. N. Voznesenskii, V. I. Nemchenko, and N. A. Samsonov, "Interaction of a severely underexpanded gas stream leaving a channel with an adjacent surface," Tr. Mosk. Fiz. Tekh., Inst. (1974).
10. E. N. Voznesenskii, V. N. Nemchenko, and N. A. Samsonov, "Some features of the action of a severely underexpanded gas stream on a flat wall," Tr. Mosk. Fiz. Tekh. Inst. (1975).